DYNAMICAL EXTENDED RANGE FORECASTING AT THE CANADIAN CLIMATE CENTRE

G.J.Boer, F.W. Zwiers and E.Chan
Canadian Climate Centre Downsview, Ontario.

1. INTRODUCTION

A series of extended range forecasts have been carried out using the Canadian Climate Centre General Circulation model. The purpose of the forecast experiment is twofold: to evaluate the systematic error of the model and to assess the skill, if any, that this low resolution model exhibits at the extended range.

The intent of this short report is to document some of the basic features of the forecast experiment. No attempt is made to compare the results obtained here with those obtained in other extended forecast studies. The papers and references in the Proceedings of the previous "Workshop on Predictability in the Medium and Extended Range" (ECMWF, 1987) serve as a basic source of information concerning previous work.

Although it is often claimed that skillful forecasts require considerably higher resolution than the T20 spectral truncation and 10 levels of this version of the CCC GCM, this assertion has perhaps not been demonstrated in general at the extended range. It may be argued that the smallest scales of the flow are very rapidly saturated with error so that skill at the extended range depends on the behaviour of the largest scales of the flow. The nature of error penetration and the generation of systematic error at these largest scales depends, in turn, on the success with which the parameterizations of the physical processes in the model are balanced with the resolution.

2. FEATURES OF THE EXPERIMENT

The features of the forecast experiment are as follows. The model used is the Canadian Climate Centre General Circulation model (Boer et al. 1984a, b) at T20L10 resolution, with both annual and diurnal cycles of radiative forcing. The model includes relatively complete parameterizations of the usual physical processes including a parameterization of gravity-wave drag. Sea surface temperatures and zonally averaged cloudiness are, however, prescribed.

Forecasts for December, January, February and July have been produced for each of the eight years from 1979 to 1986. For each month, up to six individual forecasts are made. The 6 observing periods (3 days) prior to the first day of the month provide initial conditions. All forecasts are terminated at the end of the calendar month. NMC global analyses are used both for initial conditions and as verifying data. No initialization is performed.

The boundary conditions are fixed in an "operational" way using only data available prior to the beginning of the forecast. Sea surface temperature anomalies and snow line information from the preceding week are used. The observed sea surface temperature anomaly, which is kept constant during the integration, is added to the time varying climatological sea surface temperatures of the model. The snow amount is a predictive variable in the model and evolves from its initial value as the forecast progresses.

Only the forecasts for the eight January months for 1979 to 1986 are analyzed here. Of the 48 possible forecasts (6 cases for each of the eight years), 42 were actually completed. The initial conditions were not available for the remaining 6 cases.

3. APPROACH

Attention is focussed primarily on the traditional forecast variable, Northern Hemisphere 500mb height. In particular, the anomalies of this quantity from the climatic mean must be forecast if skill is to be displayed. The "climate" from which the anomalies are calculated is the average of all NMC analyses for the eight Januaries of the study. This choice of climate is not immaterial since spuriously high anomaly correlation coefficients may arise if anomalies are calculated with respect to an inconsistent climate.

The considerable quantity of information comprising the 42 forecasts of length at least 30 days together with the verifying data must be compacted in various ways in order that it be displayed and understood. At the extended range, the basic forecast product might be considered to be the monthly mean anomaly and this is considered first. The temporal behaviour of the typical forecast is also considered by ensemble averaging the forecasts as a function of forecast time.

Let $y(\lambda, \phi, j, k, \tau)$ represent the Northern Hemisphere 500mb height forecast which is a function of latitude, longitude, year, case and forecast time. Similarly let $x(\lambda, \phi, j, \tau)$ represent the 500mb height observation. The forecast error is $e(\lambda, \phi, j, k, \tau) = y - x$. In what follows, all quantities are considered as strict functions of forecast time. Thus for a particular January, the six forecasts that are made starting from the 6 observing times preceding the first day of the month are "lined up" as functions of forecast time for subsequent averaging over years and cases.

4. BASIC STATISTICS

The decomposition of the observations and forecasts into their climatological averages and the deviations therefrom is written as

$$x_{j\tau} = \bar{x} + (x_{j\tau} - \bar{x}) = \bar{x} + x'_{j\tau}$$

$$y_{jk\tau} = \bar{y} + (y_{jk\tau} - \bar{y}) = \bar{y} + y'_{jk\tau}$$

where the overbar represents the average over all years and days of the eight Januaries for the observations and all years, cases and days for the forecasts.

The observed and forecast mean January "climate" $\bar{x}$ and $\bar{y}$ are not shown since the observed quantity is well known and the January forecast mean closely resembles the observed mean field. In any case the ability to forecast the climate has no positive skill. It is the deviation from the climate that is of interest. The inability of the forecast model to reproduce the mean January climate will, however, reveal itself in model "systematic error". The mean January systematic error defined as $\bar{e} = \bar{y} - \bar{x}$ is shown in Fig. 1. It is comparatively modest, with largest values of something in excess of 8 dm occurring over the Atlantic region.

The transient standard deviation of the observations $(\overline{x'^2})^{\frac{1}{2}}$ and of the forecasts $(\overline{y'^2})^{\frac{1}{2}}$ is shown in Fig. 2. As is typical of many forecast models, the forecast transient variability, although occurring generally in the correct geographical regions, is somewhat weaker than that of the observations.

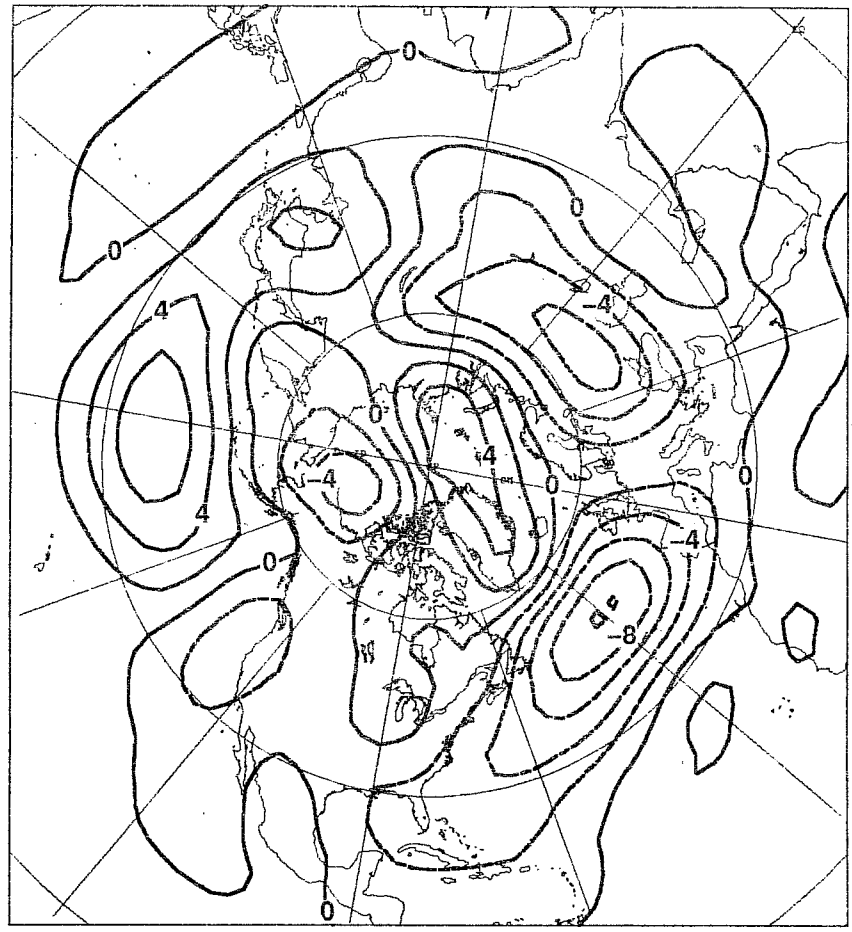

Figure 1. Mean January systematic model error for 500mb height. Units dm.

The variance of the observed 500mb height field and the corresponding error may be viewed as a function of scale by making the usual decomposition in terms of spherical harmonic expansion functions as

$$\left\langle \frac{\overline{x^2}}{2} \right\rangle = \frac{1}{4} \sum_{\alpha} \overline{|X_\alpha|^2} = \frac{1}{4} \sum_{n} \sum_{m} \overline{|X_n^m|^2} = \sum_{n} V(n)$$

$$= \frac{1}{4} \sum_{\alpha} |\bar{X}_\alpha|^2 + \overline{|X'_\alpha|^2} = \sum_{n} V_M(n) + V_T(n)$$

where the angular brackets represent an area average over the Northern Hemisphere and the overbar is again the average over all years and days for the Januaries in question. The climatological "mean" and the "transient" variance may be considered separately as shown. A similar decomposition follows for the forecast and error variance.

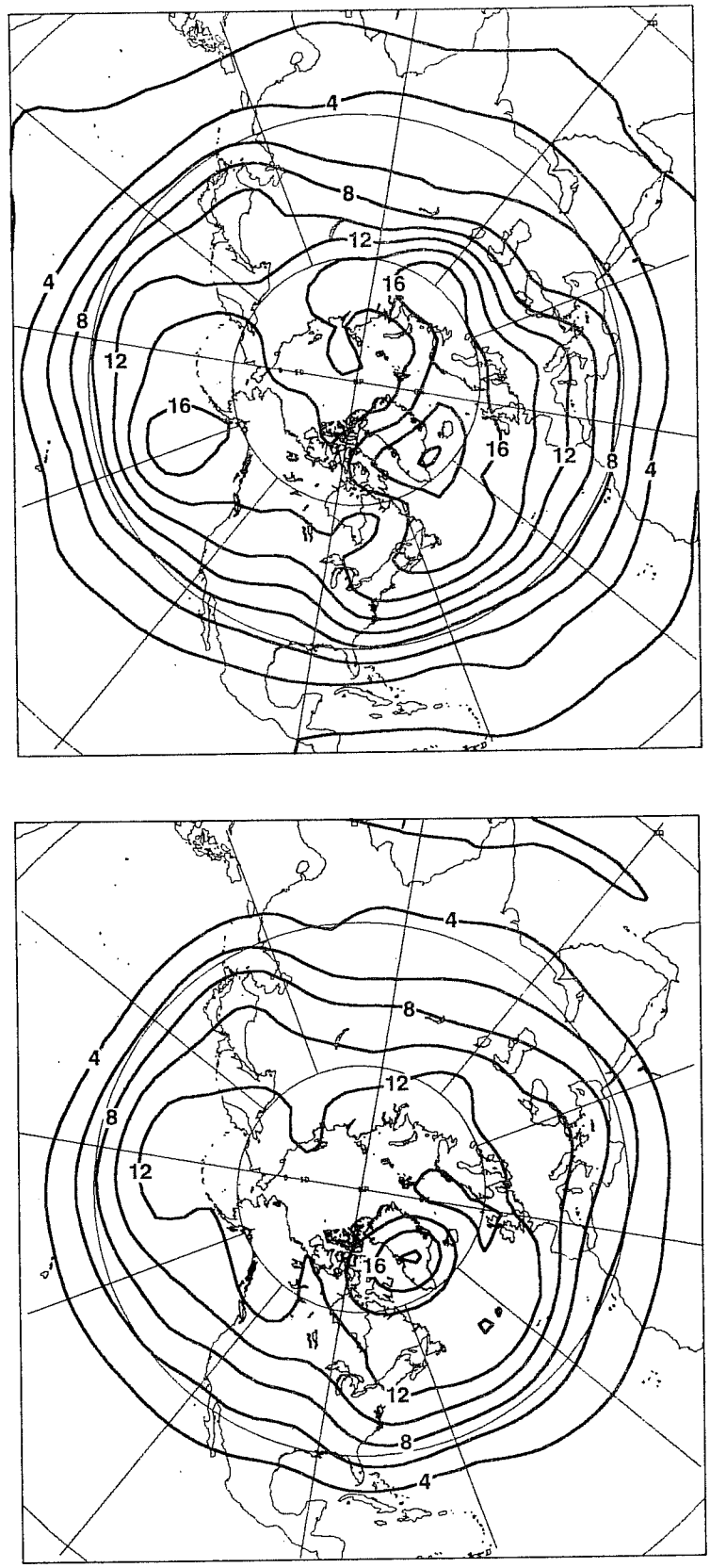

Figure 2. Observed (top) and forecast (bottom) transient standard deviation of 500mb height for January. Units dm.

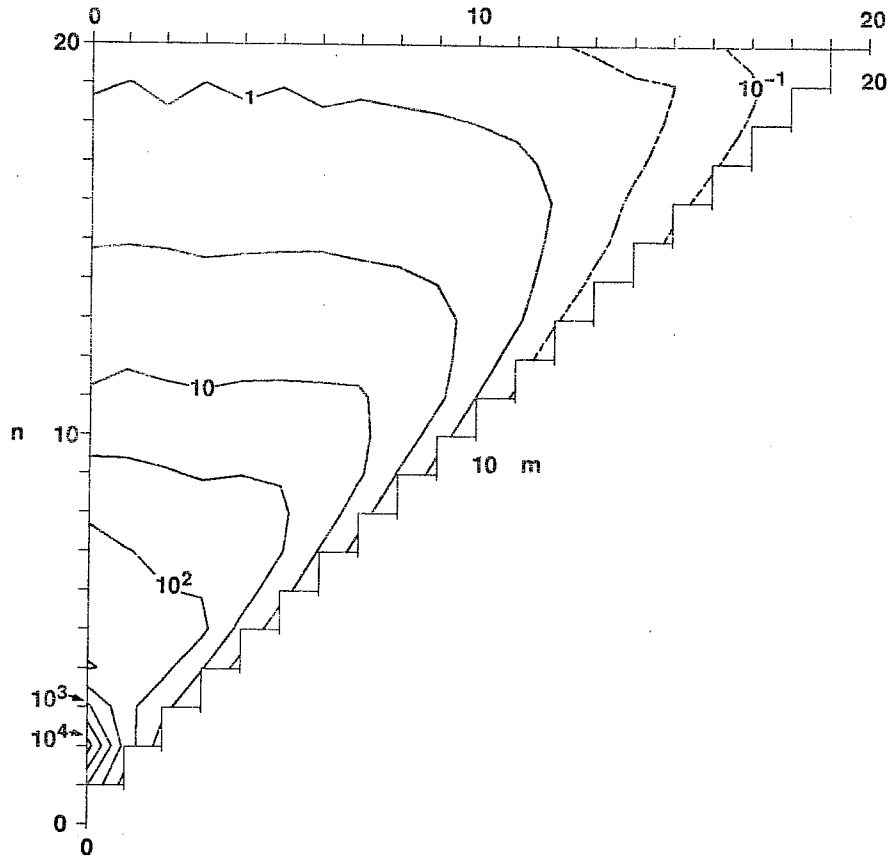

Figure 3. Variance spectrum of the observed 500mb height for January. Units m^2.

The variance spectrum of the observations is shown in Fig. 3. The largest contribution to the variance occurs at small wavenumbers and is associated with the zonal structure of the 500mb height field. These are climatological or averaged structures as opposed to the contribution to the variance from higher wavenumbers which is dominated by transients. As expected, the spectrum of the 500mb height shows the general behaviour described in Boer and Shepherd (1983) namely a low wavenumber region of large variance which is dominated by the time averaged structures and a high wavenumber region, dominated by the transients, which roughly obeys a spectral power law. This is consistent with the flow being homogeneous and isotropic at those scales.

The mean and transient error variance as a function of scale is displayed in Fig. 4. The components of the error variance are respectively the January mean systematic and non-systematic error. It is again apparent that the forecast model is quite successful in reproducing the observed climate of the 500mb height. In particular, the systematic error is rather small at low wavenumbers implying that the large amplitude zonal (m=0) structures of

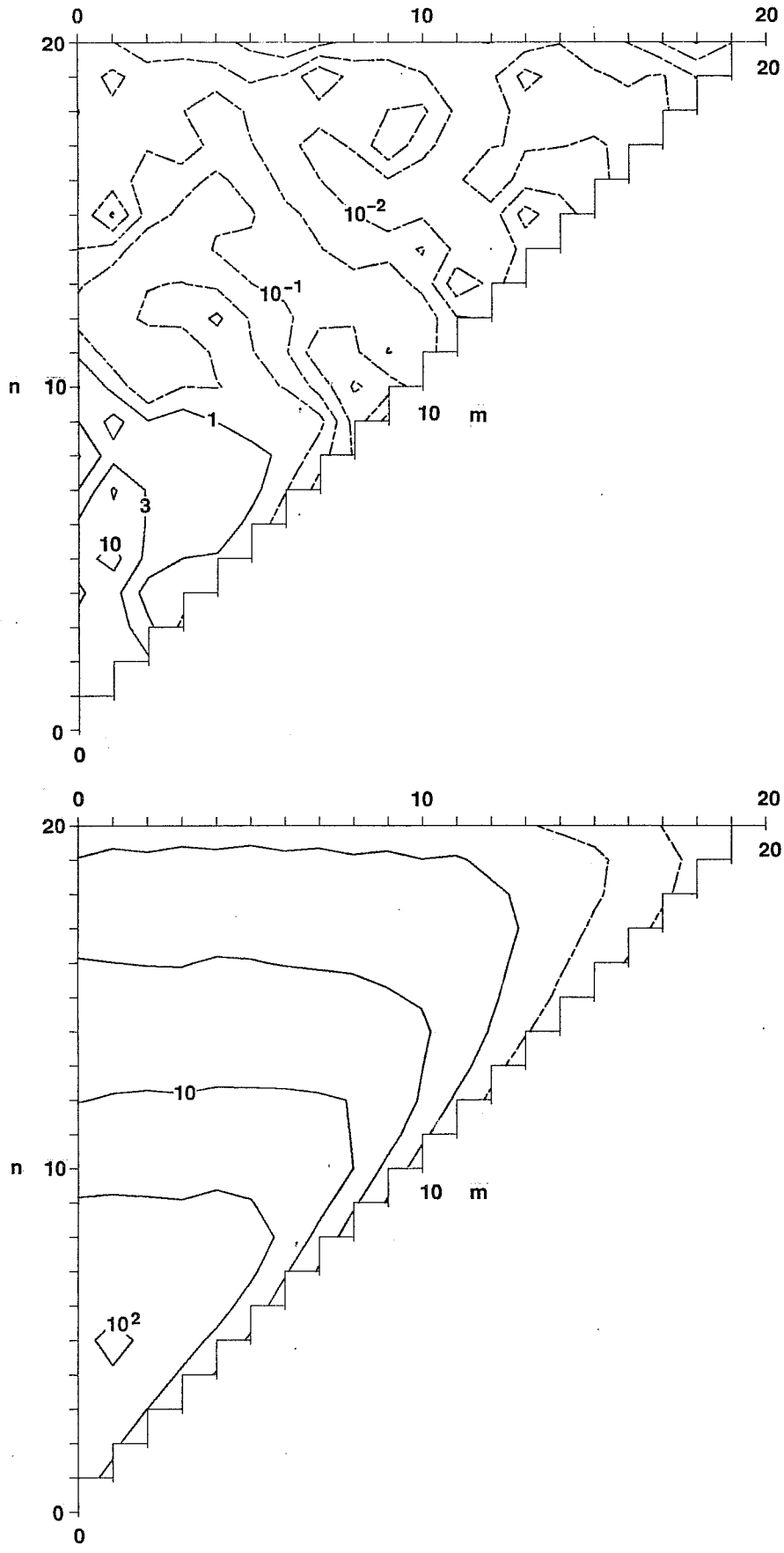

Figure 4. The systematic (top) and non-systematic (bottom) components of the January forecast error variance of 500mb height. Units m^2.

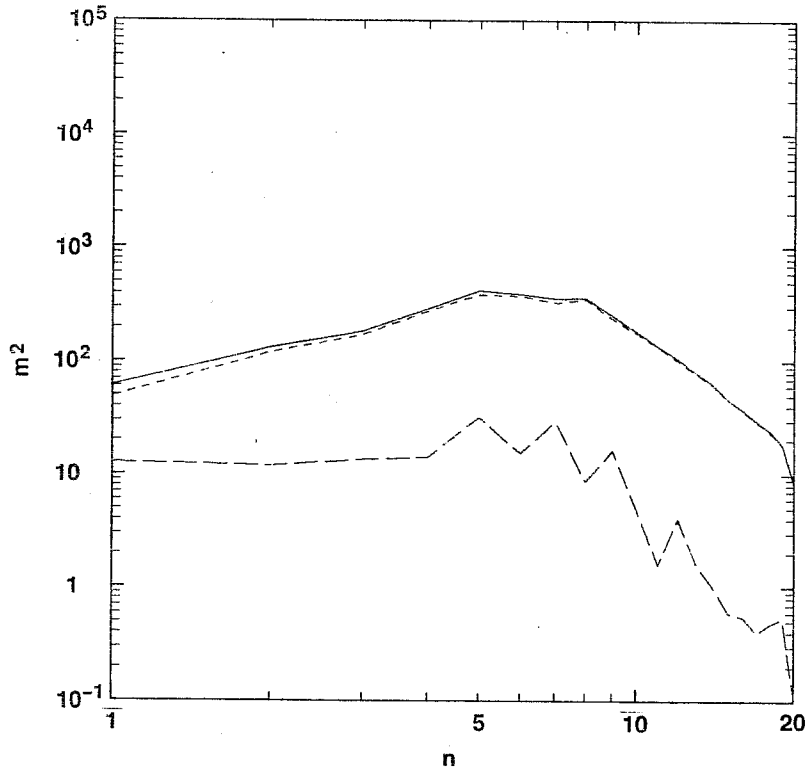

Figure 4 (continued) The corresponding n-spectrum version of the information for which the net 500mb height forecast error spectrum is the solid line, the systematic error the long dashed line and the non-systematic error the short dashed line. Units m^2.

the observed variance of Fig. 3 are well modelled. The largest systematic error variance is found for zonal wavenumber m=1 (and n=5). The systematic January forecast error for this model is perhaps distinctive in being both small and non-zonal.

The transient or non-systematic error variance is generally at least an order of magnitude larger than the systematic error. As expected, the non-systematic error shares the high wavenumber features of the observations. Finally, the n-spectrum distribution of the error variance is also shown. This points out even more clearly the comparative smallness of the systematic part and the dominance of the non-systematic part of the error at all scales.

5. REMOVAL OF SYSTEMATIC ERROR

Although the systematic error of the 500mb height field is not large, it is of interest to consider the possibility of "modelling" and removing it in some straightforward fashion. This is done by fitting simple polynomial functions $d_\alpha(\tau)$ of forecast time to the real and imaginary parts of the spherical harmonic expansion coefficients of the field. In particular the expression

$$\sum_\tau (\bar{e}_\alpha(\tau) - d_\alpha(\tau))^2 \, W_\alpha(\tau)$$

is minimized where $\bar{e}_\alpha(\tau)$ is the spherical harmonic expansion coefficient of the systematic (averaged over all years and cases) error and $W_\alpha(\tau)$ is a weight which is inversely proportional to the scatter among forecasts for the different Januaries. This weighting discounts the "average" error if the values for the individual years differ appreciably.

Figure 5 indicates the amount of the systematic error which is captured by fitting polynomials of different order to the spectral expansion coefficients up to some limit indicated by the "truncation wave number n". Based on this graph, the systematic error is modelled by fitting 4th order polynomials to spectral coefficients for which $n \leq 10$. Since the systematic error is comparatively small to begin with, it cannot be modelled with a very few coefficients and, as noted above, is not dominated by the zonal components. For this model, the correction of systematic error is not a major consideration for reducing forecast error, at least in an overall sense.

6. JANUARY MEAN FORECAST SKILL

In this section the January mean observed 500mb Northern Hemisphere height anomalies for the 8 years are indicated by x_j, the corresponding forecast anomalies as y_{jk} and the error as e_{jk}. For this case, when all variables refer to the January mean, the "ensemble mean forecast" is defined as

$$\bar{y}_j = \sum_k y_{jk}/K$$

which represents the averaging together of all the forecasts (up to 6) made for a particular year. Uniform weights are used since all forecasts are averaged together at the same forecast time. This represents an idealization of the situation in practice where the forecasts would be arranged as to calendar date and non-uniform weights applied.

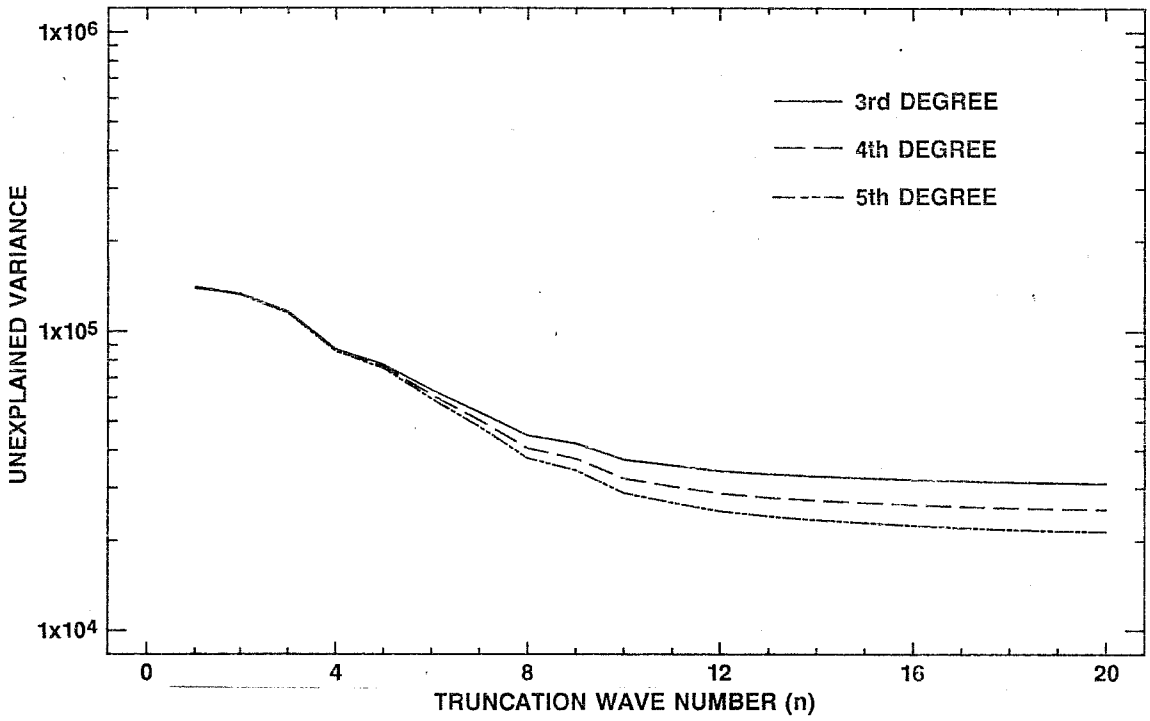

Figure 5. The effectiveness of "modelling" the 500mb height systematic error by fitting simple polynomial functions of forecast time to the spherical harmonic expansion functions.

The basic idea behind using a set of forecasts is, of course, straight forward. Averaging several samples from a random process provides a better estimate of the mean than does a single sample and the scatter among samples gives some information about the second moment of the distribution. Averaging together the several forecasts should be equivalent to applying a sophisticated temporal and spatial filter to the forecast which filters out those time and space scales which add noise but no information. In practice, it is not clear what the optimum number of forecasts (here 6) need be nor is it clear how to ensure that the several forecasts suitably explore the probability distribution.

The skill of the mean January forecasts may be judged in a number of ways. Figure 6 displays the spatial anomaly correlation coefficients

$$r_{jk} = \frac{\langle x_j \, y_{jk} \rangle}{\langle x_j^2 \rangle^{\frac{1}{2}} \langle y_{jk}^2 \rangle^{\frac{1}{2}}}$$

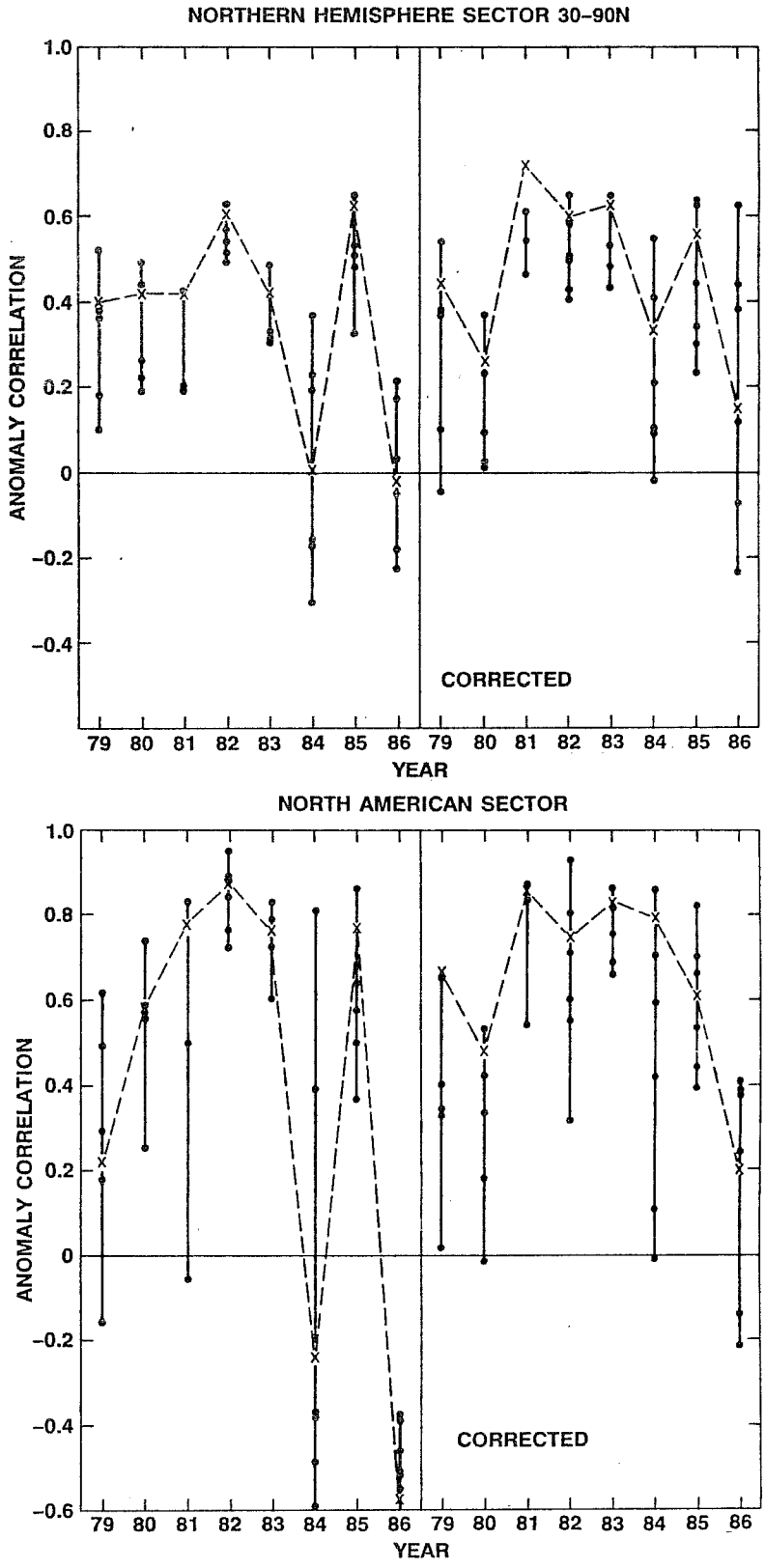

Figure 6. Anomaly correlation coefficients for mean January forecasts for (top) the Northern Hemispheric sector from 30-90N and (bottom) the North American sector 30-70N, 50-150W. Values for individual forecasts are indicated by dots while the values for the ensemble means are indicated by crosses which are also joined by dashed lines. The rightmost panel in each case gives the result after removing systematic error.

for the individual cases (dots) and for the ensemble mean forecast (crosses) both for the extratropical Northern Hemispheric region from 30-90N and the North American region 30-90N, 50-140W. The results are also given after removal of the modelled systematic error of section 5 (termed the corrected case).

For the Northern Hemispheric sector of Fig. 6, the January mean anomaly correlation for the ensemble forecast is below 0.5 in 6 of the 8 years with 1984 and 1986 clearly the worst. The removal of the systematic error generally, but not invariably, increases the values of the anomaly correlation so that, after correction, half of the years show values greater than 0.5.

For the restricted North American sector, correlation coefficients generally have larger magnitudes than for the geographically more extensive Northern Hemispheric sector. For this region, 5 of 8 of the years have ensemble mean forecast anomaly correlations which are greater than 0.5 while after correction this increases to 6 (almost 7) of the 8. Apparently, the model shows some general skill in the North American sector. Values of the anomaly correlation are generally (and perhaps surprisingly) high in this case.

A visual inspection of Fig. 6 suggests that there may be some relationship between the "spread" among the correlation coefficients for the different forecasts for the same year and the corresponding ensemble mean forecast. This is indicated specifically in Fig. 7 where the ensemble mean forecast anomaly correlation is plotted against the difference in the anomaly correlations between the largest and smallest values for each month. This "spread" is just the length of the vertical lines of Fig. 6. There are statistically significant relationships at the 5% level between ensemble mean forecast anomaly correlation and the spread among the anomaly correlations of the individual forecasts in the case of the Northern Hemisphere sector (the correlation coefficients appropriate to the least squares straight lines are -0.77 and -0.81 for the uncorrected and corrected cases). No significant relationship exists for the North American sector case.

Finally, Fig. 8 gives the mean January anomaly forecast skill at each geographical point from the relation

$$r(\lambda, \phi) = \frac{\overline{x' y'}}{(\overline{x'^2})^{\frac{1}{2}} (\overline{y'^2})^{\frac{1}{2}}}$$

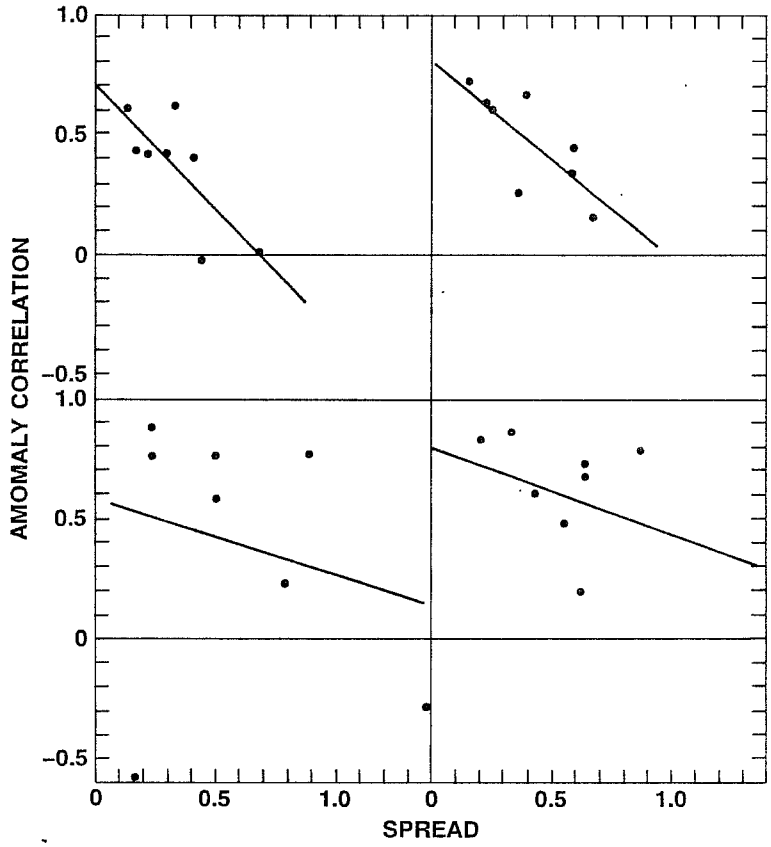

Figure 7. Plots of the anomaly correlation coefficient for the ensemble mean forecast against the spread among the individual forecasts for a particular year (this corresponds to plotting the crosses of Figure 6 against the lengths of the corresponding vertical lines indicating the spread). Regression lines are also plotted. The upper panels refer to the Northern Hemispheric sector and the lower panels to the North American sector of Fig. 6.

where $x' = x_j - \bar{x}$ and $y' = y_{jk} - \bar{y}$ and the average is over all years and cases. This correlation coefficient is not the same as the those discussed above which involve the correlation over a geographical region under area averaging. Rather, this calculation asks to what extent, at each geographical point, mean January forecast anomalies of 500mb height are accompanied by similar observed anomalies. Values greater than 0.4 are shaded in the diagram. Because of the way these correlations are calculated, the systematic error does not enter.

The correlations are, at least, generally positive (although there are small regions with negative values) but values are not high. No attempt is made here to "explain" the result in terms of "natural patterns of variability" such as the PNA or other such patterns. Visually at least there is no obvious relationship between Fig. 8 and variability measures like those of Fig. 2. There is no obvious relationship either with regions of "potential predictability" as documented for the model by Zwiers (1987). It is tempting

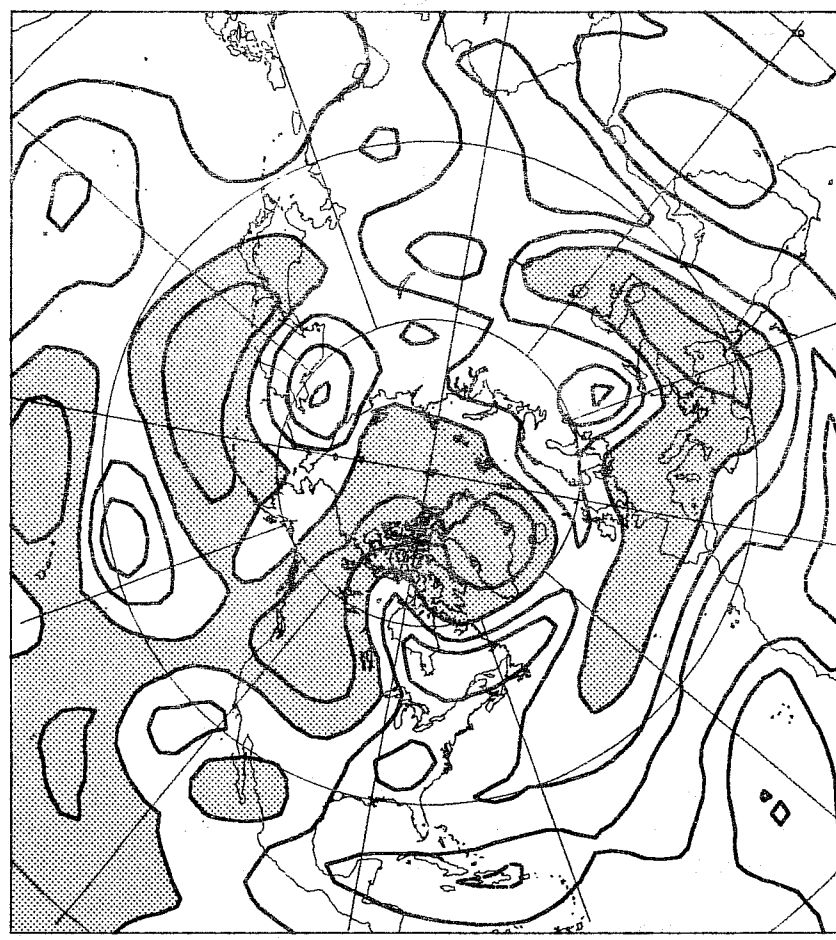

Figure 8. The geographical distribution of the anomaly correlation coefficient for January mean forecasts calculated from the 8 years of the study. The contour interval is 0.2 and negative contours are dashed. Values greater than 0.4 are shaded.

to see a connection between regions of modestly high correlation and those of high cyclone frequency in the model as documented by Lambert (1988). This would suggest that if the atmosphere develops cyclones where the model does, in a climatological sense, there is some success in the forecast. However, these comments are entirely speculative and further analysis is required to attempt to understand why this geographical pattern of forecast skill (if it should prove to exist also in the other winter months) is as it is.

To summarize the results for the forecast of the mean January anomaly of 500mb height:

i. There is apparently marginal forecast skill for the 30-90N Northern Hemispheric region as measured by the anomaly correlation coefficient. Although the systematic error is not large, when it is removed the skill level increases slightly so that half of the years display anomaly correlation values greater than 0.5 for the ensemble mean forecast.

ii. For this same region there is a statistically significant relation between ensemble mean forecast skill and the spread between the individual forecasts.

iii. For the North American region from 30-70N and 50-140W, the anomaly correlation coefficients display more extreme values and more sensitivity to the removal of systematic error. After removal of the error some 7 of the 8 years display anomaly correlations for the ensemble mean forecast of near or greater than 0.5.

iv. For the North American region there is no significant relationship between forecast skill and spread.

v. There exist geographically connected regions for which the temporal anomaly correlation (as opposed to the spatially averaged values discussed above) show modestly high values. There is no immediate relationship between these regions and obvious flow parameters.

7. FORECAST BEHAVIOUR AS A FUNCTION OF TIME

The nature of error propagation with scale must be understood if the utility of extended range forecasts is to be exploited. An understanding of error generation and propagation through the spectrum will be a prerequisite for efforts to predict forecast skill. It is intended to evaluate the various terms in the forecast error budget at long times as in Boer (1984) but at this stage only the general behaviour of error with forecast time and scale is discussed.

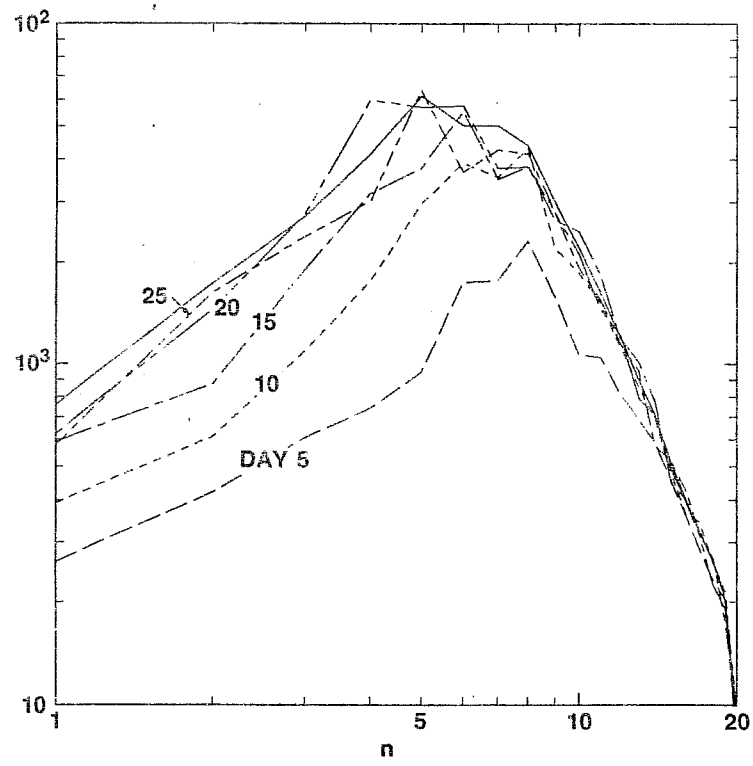

Figure 9. Error variance as a function of forecast time and scale averaged over all forecasts. The solid curve is the observed plus forecast variance.

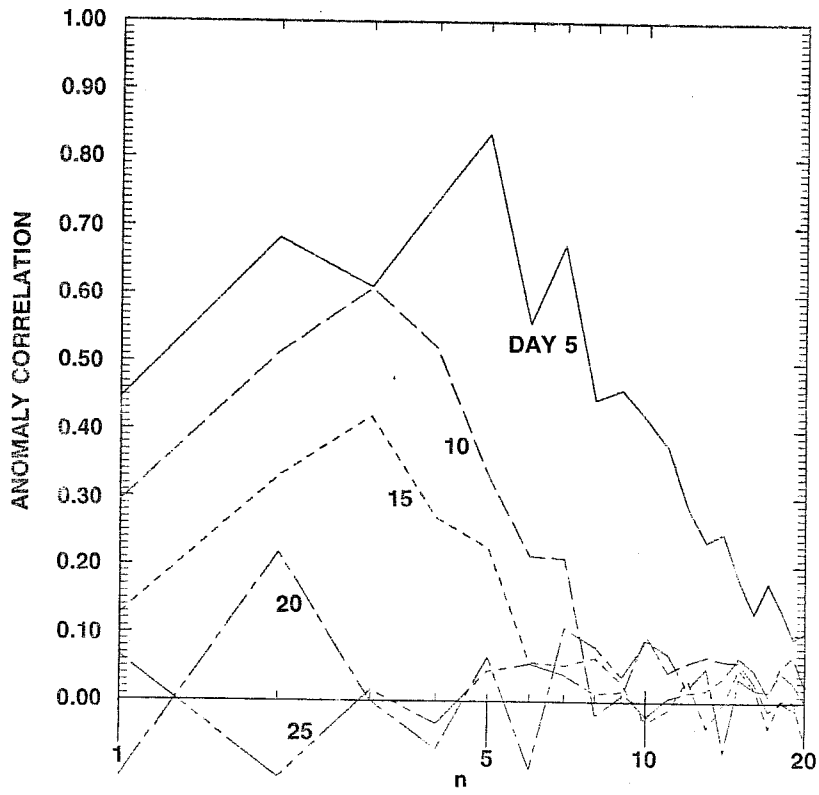

Figure 10. The spectral anomaly correlation coefficient as a function of forecast time averaged over all forecasts.

The average spectral error as a function of two-dimensional wavenumber n is expressed as

$$\left\langle \frac{e^2(\tau)}{2} \right\rangle = \frac{1}{4} \sum_{\alpha} \overline{|e_{\alpha}(\tau)|^2} = \sum_{n} E(\tau)$$

where the average is over all years and cases for the specific forecast time. Figure 9 shows the spectral error (with the estimate of the systematic error removed) at five day intervals. The solid line in the diagram is the averaged observed plus forecast variance and represents the error "saturation" level when there is not longer any correlation between the forecast and the observations. As expected, the error in the smaller scales saturates almost immediately while skill in the larger scales is lost more slowly.

The spectral anomaly correlation coefficient is plotted in Fig. 10 at 5 day intervals. Once again skill is lost quickly in the smaller scales and more slowly at larger scales. By day 20 the spectral correlation coefficient is virtually zero at all scales.

8. CONCLUDING COMMENTS

A forecasting experiment has been undertaken comprising forecasts for December, January, February and July 1979 to 1986. Only the forecasts for the 8 Januaries are analyzed. The forecast experiment uses the low-resolution Canadian Climate Centre general circulation model. Attention is confined to the "traditional" extended range variable, namely the Northern Hemisphere 500mb height field.

The systematic error of this model is comparatively small for January. The zonal component is well forecast so the largest contribution is not from this component. The contribution of the systematic error to the total error is an order of magnitude smaller than that of the non-systematic error. The systematic error as a function of time is "modelled" by fitting fourth order polynomials to low order spectral coefficients.

The skill of the mean January anomaly forecast as measured by the anomaly correlation coefficient is in the vicinity of 0.5 for the Northern Hemispheric region from 30-90N. Correction for the systematic error makes only a modest improvement in the scores. There is a statistically significant relationship between the value of the ensemble mean forecast anomaly coefficient and the spread of the (up to 6) forecasts for the same January which suggests that some information concerning the goodness of the forecast may be available.

The skill of the mean January anomaly forecast for the North American region is surprisingly high especially after correction for the systematic error. In this case the ensemble mean forecast correlation coefficient is near or greater than 0.5 for 7 of 8 years. There is no clear connection between forecast skill and spread in this case.

Finally, the propagation of the error through the spectrum with time displays the expected behaviour with error dominating the small scales early in the forecast but requiring more time to penetrate the larger scales. Clearly the possibility of skillful extended range forecasting resides in the behaviour of these large scales. The sources of error at these scales, methods of correcting for this error and the prior knowledge of atmospheric states for which these scales are shielded from error are all areas of further analysis of this forecast experiment.

ACKNOWLEDGEMENTS

We would like to thank Lynda Smith who aided in the production of the manuscript and Brian Taylor with the figures.

References

Boer, G.J. and T.G. Shepherd, 1983: Large-scale two-dimensional turbulence in the atmosphere. J. Atmos. Sci., 40, 164-184.

Boer, G.J., N.A. McFarlane, R. Laprise, J.D. Henderson, and J.-P. Blanchet, 1984a: The Canadian Climate Centre spectral atmospheric general circulation model. Atmos.-Ocean, 22, 397-429.

Boer, G.J., N.A. McFarlane, and R. Laprise, 1984b: The climatology of the Canadian Climate Centre general circulation model as obtained from a five-year simulation. Atmos.-Ocean, 22, 430-475.

Boer, G.J., 1984: A spectral analysis of predictability and error in an operational forecast system. Mon. Wea. Rev., 112, 1183-1197.

ECMWF, 1987: Workshop on predictability in the medium and extended range. European Centre for Medium Range Forecasting, Shinfield Park, U.K., pp 414.

Lambert, S.J., 1988: A cyclone climatology of the Canadian Climate Centre general circulation model. J. Clim., 1, 109-115.

Zwiers, F.W., 1987: A Potential Predictability Study Conducted with an Atmospheric General Circulation Model. Mon. Wea. Rev., 115, 2957-2974.